

On the near-infrared halo of Elias 1

Martin Haas¹, Christoph Leinert¹, and Andrea Richichi²

¹ Max-Planck-Institut für Astronomie, Königstuhl 17, D-69117 Heidelberg, Germany

² Osservatorio Astrofisico di Arcetri, Largo E. Fermi 5, I-50125 Firenze, Italy

Received 20 January 1997 / Accepted 2 June 1997

Abstract. We present new near-infrared speckle interferometric observations of the young stellar object Elias 1. The emission is resolved into a narrow east-west elongated blue halo (FWHM about $0''.2 \times 1''.0$) and an unresolved core (FWHM $< 0''.2$). Previously, Kataza and Maihara (1991) had inferred an east-west elongated optically thin disk within which the NIR light is directly scattered. Adding new pieces to the puzzle may alter the scenario in favor of scattering in bipolar lobes with a polar axis oriented east-west.

Key words: stars: pre-main sequence – stars: circumstellar matter – stars: Elias 1 – infrared: stars

1. Introduction

Elias 1 has been proposed as illuminating source of the nebulosity IC 359 located in the Taurus-Auriga complex and was classified as Herbig Ae star (Elias, 1978). The extinction has been estimated between $A_v = 8.85$ mag (Strom and Strom, 1994), $A_v = 6.1$ (Berilli et al., 1992) and $A_v = 3.9$ mag (Zinnecker and Preibisch, 1994). Still, no deep optical images are known and thus it is not clear, whether Elias 1 has a jet. Using a small (4.9 m) antenna Levreault (1988) searched for a molecular outflow, but without detection. In the near infrared the SED is rising with wavelength. From continuum observations at 1.3 mm Beckwith et al. (1990) inferred the presence of a circumstellar disk.

By NIR speckle interferometry Kataza and Maihara (1991) resolved Elias 1 at K and L' into an unresolved core and a sub-arcsec structure elongated in east-west direction. Accounting for the north-south orientation of the NIR polarisation (Moneti et al. 1984; Tamura and Sato, 1989) they interpreted the light of the east-west elongated structure as being reflected within an edge-on circumstellar disk of moderate optical depth. This is a remarkable interpretation which would give direct evidence of a circumstellar disk seen in the NIR.

Here we present new NIR speckle results covering a larger wavelength range from J to L' and going to higher resolution.

Send offprint requests to: M. Haas

From these data we suggest that the east-west elongated structure is due to light scattered from bipolar lobes rather than from the disk itself.

2. Observations

The observations were performed during several campaigns in September 1986, February 1992 and January 1993 using the 1D specklegraph at the 3.5 m telescope on Calar Alto. Briefly, fast slitscans are obtained with an In Sb photodiode, yielding 1D specklegrams (Leinert and Haas, 1989). Typically, an observation consisted of 1000 scans of about 100 ms on the object as well as on a nearby pointlike reference star, and of a similar number of background exposures next to them. We performed observations with the slit oriented north-south and east-west. The seeing was $1-2''$.

3. Data reduction

As usual, the application of speckle data reduction techniques results in the complex visibility of the object (Fourier transform of the object brightness distribution), where the modulus was determined from power spectrum analysis and the phase with the bispectrum (Lohmann et al. 1983) formalisms. The matching of the seeing conditions for object and reference star was checked and slightly improved using the sorting criteria developed by Haas (1989).

4. Results

Fig. 1 shows the normalised visibility modulus for different wavelengths and position angles. The phases are not shown since they were always close to zero indicating rather symmetric flux distributions for each position angle.

We consider first the visibility at J and H: At PA 90° the visibility shows a strong decrease with spatial frequency which becomes quite constant for the frequencies higher than $1.0/\text{arcsec}$. The decrease corresponds to a well resolved structure (FWHM about $1''$), while the constant plateau represents an unresolved source which is well constrained at H, less so at J. The flux contribution of the resolved structure is stronger at J (20%) than at H (12%). At PA 0° the J and H visibilities are rather constant,

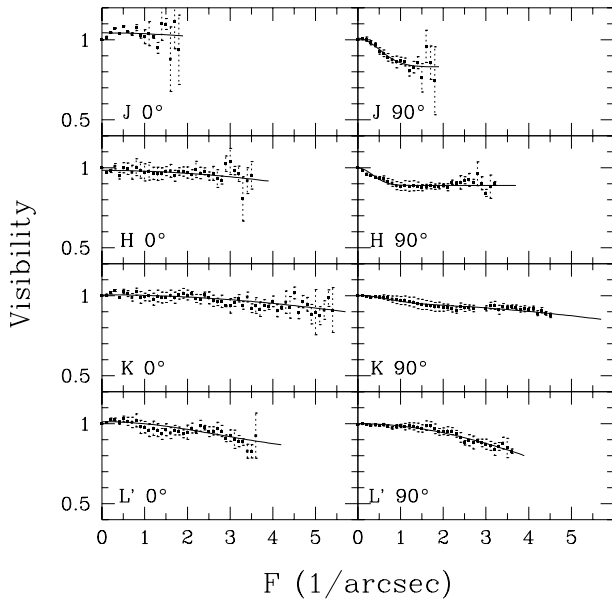


Fig. 1. Visibility of Elias 1 at different wavelengths and position angles. The crosses with error bars represent the data, the drawn lines correspond to gaussian decompositions

i.e. Elias 1 is unresolved or at best marginally resolved in this direction ($\text{FWHM} \leq 0''.2$). Hence the structure resolved at PA 90° is of narrow elongated shape with axis ratio about 5:1 and has a blue color relative to the central source.

Before continuing with the K and L' data let us briefly address the effective resolution: For our data in Fig. 1 the formal resolution limits are at about spatial frequency 2 (at J), 3 (at H), 5 (at K) and 3.5 (at L') per arcsec. This means they are different at the various wavelengths, and due to both the faintness of the source and the detector noise they do not reach the diffraction limit of the telescope of e.g. $D/\lambda = 10/\text{arcsec}$, $\lambda/D = 0''.1$ at H. Since our one dimensional data integrate the object brightness distribution along the slit, they can only exhibit simple steady brightness profiles like gaussians. And such a structure - even if narrow - shows its typical signatures already at lower spatial frequencies, which means that some reliable extrapolation to higher frequencies is possible. For example in the data at H and PA 90° , we have a clear decrease in the first spatial frequencies (until $1.0/\text{arcsec}$) followed by a constant plateau. Note that due to the calibration with the reference star the effect of the point spread function is cancelled in the visibility, hence we obtain a constant plateau and the formal resolution depends only upon the highest spatial frequencies reached. If this constant plateau represents a resolved component with $\text{FWHM} = x$ arcsec, then its visibility decreases steadily at higher frequencies, the decrease being of gaussian shape reaching the zero level to a first approximation at spatial frequency $f = 1/x$ (see also Fig. 1 in Leinert et al. 1994). For comparison, in Fig. 1 the drawn line fit at H PA 0° corresponds to a gaussian of $\text{FWHM} = 0''.036$, while the fit at L' PA 90° corresponds to $0''.065$. From these curves we infer that the effective resolution is certainly better than the formal resolution limit of $0''.3$ at H corresponding to the highest observed

spatial frequencies about $3/\text{arcsec}$. To compare the PA 90° J and H data which are quite similar in the more extended structure causing the fall-off at low spatial frequencies, we assume that the narrow component at H may also be identified with that at J. (Admittedly at frequencies between 2 and 5 per arcsec the visibility could decrease steeper in J than in H.) At PA 0° , however, the visibilities remain quite constant for both wavelengths even at the low frequencies, indicating again the similarity of the underlying components. In any case the decomposition into two components remains similar for both colors. Finally, we adopted $0''.2$, i.e. the telescope diffraction limit at L' as common effective resolution.

Considering the visibility at the longer wavelengths K and L' yields a bit different picture than at J and H: The separation into two components, one broad resolved and one unresolved is not clearly present. Instead, for both PA the K and L' visibilities show a slow decrease with spatial frequency, i.e. there is a marginally resolved component. For K and L' the visibility is decreasing slightly steeper at PA 90° than at 0° . This means that also at K and L' the resolved structure is slightly elongated in east-west direction. Note that we reach higher spatial resolution at K and L' than at J and H, thus the component unresolved at J and H may be identical with the slightly resolved structure at the longer wavelengths.

Remarkably the decrease is slightly steeper at L' than at K indicating that the structure is little more extended at L', or alternatively under the assumption that it has the same spatial extent as at K, its flux contribution would be larger in L', i.e. its color would be redder than that of the contribution of the unresolved central source.

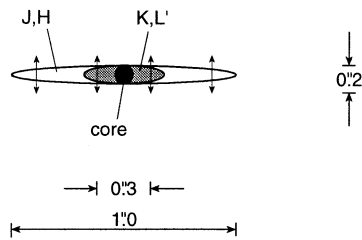
Qualitatively our results at K and L' agree with those of Kataza and Maihara (1991), although in their data the resolved structure appears more extended and more prominent at PA 90° , a fact already pointed out by Leinert et al. (1994). Note that Kataza and Maihara presented the power spectrum instead of the visibility in order to enhance the features. The remaining differences between the data could be explained by the different instruments (Kataza and Maihara used a one dimensional array at a 2.2 m telescope, while we used slit scans at a 3.5 m telescope), the errors and taking into account possible variability of the object between December 1988 (Kataza and Maihara) and January 1993 (our K and L' observations). In this comparison we consider it a strong point of our data that they extend to higher spatial frequencies.

To summarise, at J and H we see two components, one well resolved narrow blue structure elongated in the east-west direction and one marginally resolved, while at K and L' we see one more circular symmetric, marginally resolved red structure.

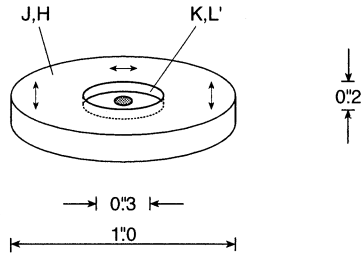
5. Discussion

We consider the origin of the emission in the framework of a disk/lobe geometry and discuss from which component - disk or lobes - the emission arises. In Sect. 5.1 we follow first the interpretation of Kataza and Maihara and try to embed our additional J and H results into their picture of scattering in an optically thin

a) edge-on disk



b) inclined disk



c) bipolar lobes

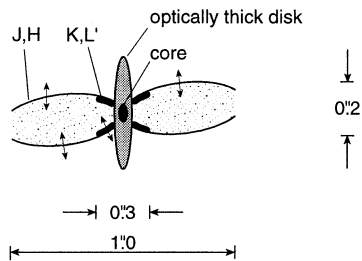


Fig. 2a–c. The various scenarios for the origin of the scattered NIR light discussed in Sects. 5.1 and 5.2. The thin double arrows indicate the orientation of the polarisation

disk seen more or less edge-on (Fig. 2a and b). Then, since we end up with difficulties, in Sect. 5.2 we discuss the alternative - quasi opposite - picture of scattering in bipolar lobes (Fig. 2c).

For both cases we assume that the polarisation measured for Elias 1 arises from scattering in the circumstellar material and not in the foreground by differential extinction. Admittedly, the polarisation degree can be well fitted by a Serkowski-Wilking law with maximum 5.4% at $\lambda=0.8 \mu\text{m}$ (Fig. 3) and the polarisation angle of PA 180° may be viewed as being aligned to that of the surrounding stars (see e.g. Moneti et al. 1984, Tamura and Sato 1988, Goodman et al. 1990, Whittet et al. 1992). But the blue color of the halo at J and H relative to the central source clearly supports the circumstellar origin. We just mention that the difficulties we encounter below are not caused by the assumption that the polarisation mechanism is assumed to be scattering.

Finally in Sect. 5.3 we discuss the nature of the L' emission, where the resolved structure appears relatively red and/or more extended (than at K).

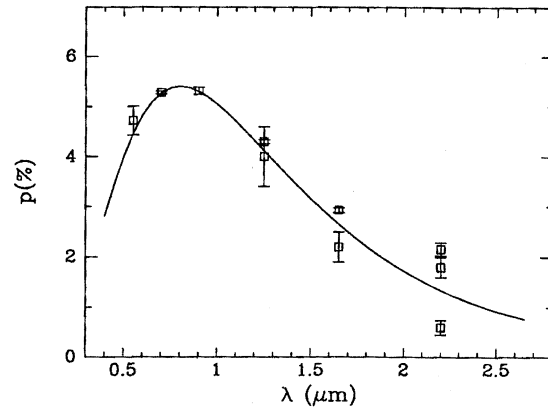


Fig. 3. Polarisation measurements on Elias 1 (squares) compared to a Serkowski-Wilking curve for interstellar polarisation with $p = 5.4\%$ and at $\lambda=0.8 \mu\text{m}$. The polarisation angle is 180° at all wavelength. The data are taken from Moneti et al. (1984), Tamura and Sato (1989) and Whittet et al. (1992)

5.1. Scattering in the disk

The arguments mentioned by Kataza and Maihara in favor of an east-west optically thin edge-on disk are the elongation in this direction, the assumption that the axis of a bipolar YSO is generally aligned parallel to the magnetic field and the acceptance of a north-south orientation of the local magnetic field from the surrounding polarimetry. The remarkable feature is that the polarisation angle is perpendicular to the disk plane. Embedding our data into this scenario means: The resolved structure at K and L' as well as the elongated one at J and H both arise from scattering within an east-west oriented disk/torus of about $1''$ (140 AU) extension (Fig. 2a). But we do not feel comfortable with this interpretation.

Calculations of scattering models by Whitney and Hartmann (1992, 1993) and Fischer et al. (1994, 1996) show that for optically thin edge-on disks the central source by far dominates the contribution of the reflected light which is less than 1% of the total flux. Though this does not contradict our K and L' observations, at J and H the observed halo contribution is clearly higher. Additional difficulties arise from the extinction which is determined to $A_v = 4-9 \text{ mag}$. In the case of reflected light this represents only a lower limit, i.e. the true extinction is higher than estimated. $A_v = 4-9 \text{ mag}$ corresponds to 1-2.5 mag at J, a value still too high to fit into the scenario of an optically thin scattering disk.

Optically thick edge-on circumstellar disks were, in fact, detected with the HST using two strategies. One is in the Orion region (McCaughrean and O'Dell, 1996), where the disks were seen in absorption on a bright background illuminated by a nearby O star. The other example is the flaring disk (surface) around HH 30 in Taurus (Burrows et al. 1996), where the polarisation, however, is parallel to the disk. In both cases the situation does not apply for Elias 1.

If the near infrared scattering occurs within the inner walls of an optically thick disk/torus leading to a polarisation angle

parallel to the bipolar axis, Bastien (1987) has already suggested a switch of the polarisation angle by about 90° for the shorter wavelengths, because of scattering in the lobes or multiple scattering at the disk surface (Bastien and Menard, 1988 and 1990). For Elias 1, however, we do not see such a switch of the polarisation angle from 0.5 to $2.2 \mu\text{m}$. In addition, one might have difficulties to imagine an optically thick edge-on torus scenario in which the radiation at shorter wavelengths J and H penetrates the torus much farther than at K and L'. Thus the case of an edge-on disk may be rejected.

Considering the case of an inclined disk (Fig. 2b) the scattering model calculations mentioned above still indicate some elongation. Nevertheless we have to deal with the polarisation angle. To reproduce a polarisation perpendicular to the disk the models require a geometrically flat disk. A thick disk or a more spherical symmetric envelope does not reproduce the observed integrated polarisation angle. Submillimetre observations, however, by Beckwith et al. (1990) and Mannings (1994) clearly indicate that Elias 1 belongs to the group II of Hillenbrand et al. (1992) with flat or rising IR SEDs. As pointed out by Mannings the circumstellar dust of a group II system subtends a solid angle larger than that of a flat disk. A similar conclusion was also derived from far-infrared data for other Herbig Ae/Be stars by Natta et al. (1993).

Near infrared adaptive optics imaging of the inclined system HL Tau (Close et al. 1997) revealed a faint disk which, however, is clearly (by a factor about 100) dominated by the emission of the bipolar halo. If Elias 1 had an inclined disk, we would expect to see also a dominant (bipolar) near infrared halo.

To summarise, there remain several objections against the interpretation that the resolved elongated structure originates from scattering in an east-west disk. Therefore we consider now an alternative interpretation.

5.2. *Elias 1 as a bipolar nebula*

In this picture the resolved elongated structures at J and H arise from scattering in the bipolar lobes which probably are hollow cavities whose axis lies in the plane of the sky. This allows easily to explain the polarisation angle and degrees observed in the optical and near infrared (cf. Elsässer and Staude, 1978). Also the blue J-H color of the halo compared with the unresolved core fits into this picture as well as the decrease of the halo contribution and extension from J and H to K.

Similar cases of blue scattering near infrared haloes were already observed for HL Tau (Beckwith et al. 1989), Lk H α 198 and V376 Cas (Leinert et al. 1991) and GL 490 (Haas et al. 1992). These nebulae, however, are not as strongly elongated as Elias 1. This fact also led Kataza and Maihara to reject the bipolar lobe scenario. Nevertheless there exist small strongly elongated bipolar nebulae, e.g. the source number 22 in the compact region around HH34 where several bipolar nebulae with different orientations are found (Reipurth 1985, Bührke et al. 1988, Scarrott 1988). Therefore we see no objection against the bipolar lobe interpretation for the J, H and K data and consider it at least as attractive as the disk interpretation.

Finally we consider the orientation of a bipolar axis with respect to the surrounding magnetic field. Submillimetre and CO aperture synthesis imaging of some YSOs in Taurus by Koerner and Sargent (1995) (RY and DL Tau) and Jensen et al. (1996) (UZ Tau) reveal rotating disks of about $1''$ extension. Remarkably for all these sources the optical and NIR polarisation angles turn out to be parallel to the disk and not to the bipolar axis. This is even the case, when the polarisation has similar orientation for the source as for the surrounding region. Obviously there exist counter examples to the suggestion that the bipolar axis is always parallel to the direction of the surrounding optical polarisation, i.e. magnetic field. In addition, the magnetic field direction is not well determined in the region around Elias 1. It reveals some curvature: southwards of Elias 1 it is aligned east-west, but eastwards it is aligned more north-south (see e.g. Moneti et al. 1984, Tamura and Sato 1988, Goodman et al. 1990, Whittet et al. 1992). Note that we do not doubt that the magnetic field might play an important role in aligning the bipolar axis, but probably the orientation of the magnetic field has local distortions not inferrable from a few polarisation values of the surrounding stars which may be far away, as was clearly demonstrated by Goodman et al. (1990).

5.3. *Nature of the L' band emission*

The visibility drops more at L' than at K. This is not the signature of scattering. Our data, however, do not reach sufficiently high spatial resolution to define the origin of the extended L' emission. Therefore we consider two possible alternatives of thermal emission, an inner envelope which has relatively red color or an infrared companion. We discuss both alternatives starting with the companion, but each of them will leave us with open questions.

The visibility decrease at K and L', PA 0° and 90° , could well be fitted by a close binary which would be oriented about PA 45° or 135° (separation $< 0''.1$, brightness ratio = 0.08 ± 0.04 at K and 0.2 ± 0.1 at L', up to our resolution the binary fits are not distinguishable from those of a gaussian fit shown in Fig. 1). Then Elias 1 would be unresolved in one of these directions. The SED of such a binary would resemble that of an infrared companion like those found for Z CMa (Koresko et al. 1991, Haas et al. 1993) or for XZ Tau (Haas et al. 1990). This possibility appears very attractive to us since it allows easily to explain the quite red K-L' color compared with the rather blue J-H and H-K halo colors of the halo. At J and H such an infrared companion could be very faint and too close for our spatial resolution. (Note that Elias 1 has a known faint companion located about $5''$ northwest, i.e. rather far away. Its NIR properties have already been discussed by Leinert et al. (1997). Here we consider the possibility of a very close infrared companion.)

As mentioned above we have not performed observations along PA 45° and 135° . However, there are additional observations at L' presented by Kataza and Maihara which indicate that Elias 1 is also resolved at PA 45° and 135° . This is not the signature expected for a companion, rather it indicates the presence of circumstellar diffuse distribution of matter. But this fact does

not exclude a possible infrared companion in addition to some extended structure. The definite detection of a close companion, however, might have to await the better spatial resolution obtained with new large telescopes.

Next we consider thermal emission from an inner dust halo. Elias 1 has about 38 solar luminosities (see Leinert et al. 1997). The K-L color temperature corresponds to about 500-1000 K. This temperature range might only be reached within 1-3 AU from the central star. The extension of an inner dust halo, however, is of the order of $0''.05-0''.1$, i.e. 7-14 AU. At these distances from the central star the temperature of emitting dust would be expected to be much lower. Thus simple thermal emission appears not attractive to us. A similar argumentation was given by Malbet et al. (1993) for the 400 AU disk around Z CMa, in order to exclude thermal emission as source of the disklike structure found in the L and M bands. Note, that for Z CMa the situation is different from that of Elias 1: there is a known second light source in the system, the cool close companion star, which is not known for Elias 1.

Another explanation in favor of the inner dust halo alternative is based on an unusual grain size distribution and composition, different from the interstellar MRN-like one (Mathis et al. 1977). Prominent infrared spectral features between 3 and 4 μm have been reported for Elias 1, in particular those at 3.42 and 3.53 μm (e.g. see Schutte et al. 1990, Tokunaga et al. 1991 or Brooke et al. 1993). Our L' filter at $3.69 \pm 0.315 \mu\text{m}$ includes these bands which are believed to be correlated to aromatic hydrocarbonates (PAHs). Such molecules are probably destroyed in the presence of a strong UV radiation field (for a review see Puget and Leger 1989), like that we expect very close to the A6 star Elias 1. At some distance from the star, however, PAHs and very small grains could survive. They would then be heated sufficiently and radiate via fluorescence. In this picture the inner dust halo resolved at L' would owe most of its thermal 3-4 μm emission to the presence of non-standard grain composition in the surrounding of Elias 1.

To summarise, thermal emission could be a viable explanation for the resolved structures and the red colors in K and L'. Scattering would still dominate in J and H, resulting in blue colors.

Acknowledgements. We thank the Calar Alto staff for their classical support during our observations and Reinhard Mundt, Marc McCaughrean, Robert O'Dell and Jakob Staude for fruitful discussions and the referee Francois Menard for his constructive criticism.

References

- Bastien P. 1987, ApJ 317, 231
 Bastien P., Menard F. 1988, ApJ 326, 334
 Bastien P., Menard F. 1990, ApJ 364, 232
 Beckwith S.V.W.B., Sargent A.I., Chini R.S., Güsten R. 1990, AJ 99, 924
 Beckwith S.V.W.B., Sargent A.I., Koresko C.D., Weintraub D.A. 1989, ApJ 343, 393
 Berilli F., Corciulo G., Ingrassio G., Lorenzetti D., Nisini B., Strafella F. 1992, ApJ 398, 254
 Brooke T.Y., Tokunaga A.T., Strom S.E. 1993, AJ 106, 656
 Bührke Th., Mundt R., Ray T.P. 1988, A&A 200, 99
 Burrows C.J., Stapelfeldt K.R., Watson A.M. et al. 1996, ApJ 473, 437
 Close L.M., Roddier F., Northcott M.J., Roddier C., Graves J.E. 1997, ApJ 478, 766
 Elias J.H. 1978, ApJ 224, 857
 Elsässer H., Staude J. 1978, A&A 70, L3
 Fischer O., Henning Th., Yorke H.W. 1994, A&A 284, 187
 Fischer O., Henning Th., Yorke H.W. 1996, A&A 308, 863
 Goodman A.A., Bastien P., Myers P.C., Menard F. 1990, ApJ 359, 363
 Haas M. 1989, A&A 236, 531
 Haas M., Christou J.C., Zinnecker H., Ridgway S.T. Leinert Ch. 1993, A&A 269, 282
 Haas M., Leinert Ch., Lenzen R. 1992, A&A 261, 130
 Haas M., Leinert Ch., Zinnecker H. 1990, A&A 230, L1
 Hillenbrand L.A., Strom S.E., Vrba F.J. Keene J. 1992, ApJ 397, 613
 Jensen E.L.N., Koerner D.W., Mathieu R.D. 1996, AJ 111, 2431
 Kataza H., Maihara T. 1991, A&A 248, L1
 Koerner D.W., Sargent A.I. 1995, AJ 109, 2138
 Koresko C.D., Beckwith S.V.W.B., Ghez A., Matthews K., Neugebauer G. 1991, AJ 102, 2073
 Leinert, Ch., Haas, M. 1989, A&A 221, 110
 Leinert, Ch., Haas, M., Lenzen R. 1991, A&A 246, 180
 Leinert, Ch., Richichi A., Weitzel N., Haas M. 1994, in 'The nature and evolutionary status of Herbig Ae/Be stars', eds. P.S.Thé, M.R.Pérez and Ed P.J van den Heuvel, Astron. Soc. Pac. Conf. Ser 62, p.155
 Leinert, Ch., Richichi A., Haas M. 1997, A&A 318, 472
 Levreault, R.M. 1988, ApJ 330, 897
 Lohmann, A.W., Weigelt, G., Wirmitzer, B. 1983, Appl. Opt. 22, 4028
 Mannings V. 1994, MNRAS 271, 587
 Mathis J.S., Rumpl W., Nordsieck K.H. 1977, ApJ 217, 425
 Moneti A., Pipher J.L., Helfer H.L., McMillan R.S., Perry M.L. 1984, ApJ 282, 508
 McCaughrean M. J., O'Dell C. R., 1996, AJ 111, 1977
 Natta A., Palla F., Butner H.M., Evans II N.J., Harvey P.M. 1993, ApJ 406, 674
 Puget J.L., Leger A. 1989, ARAA 27, 161
 Reipurth B. 1985, ApJS 61, 319
 Scarrott S.M. 1988, MNRAS 231, 1055
 Schutte W.A., Tielens A.G.G.M., Allamandola L.J., Cohen M., Wooden D.H. 1990, ApJ 360, 577
 Strom K.M., Strom S.E. 1994, ApJ 424, 237
 Tamura M., Sato S. 1989, AJ 98, 1368
 Tokunaga A.T., Sellgren K., Smith R.G. et al. 1991, ApJ 380, 452
 Whitney B.A., Hartmann L. 1992, ApJ 395, 529
 Whitney B.A., Hartmann L. 1993, ApJ 402, 605
 Whittet D.C.B., Martin P.G., Hough J.H., Rouse M.F., Bailey J.A., Axon D.J. 1992, ApJ 386, 562
 Zinnecker H., Preibisch Th., 1994, A&A 292, 152